LA-UR-02-1690
Approved for public release; distribution is unlimited.

Title: **Large Scale Statistics for Computational Verification of Grain Growth Simulations with Experiments**

Author(s): Melik C. Demirel, Andrew P. Kuprat, Denise C. George, Galen K. Straub, Amit Misra, Kathleen Alexander and Anthony D. Rollett

Submitted to:

http://lib-www.lanl.gov/cgi-bin/getfile?00852308.pdf

Mat. Res. Soc. Symp. Proc. Vol. 731 © 2002 Materials Research Society

Large Scale Statistics for Computational Verification of Grain Growth Simulations with Experiments

Melik C. Demirel[1,2,3], Andrew P. Kuprat[2], Denise C. George[2], Galen K. Straub[2], Amit Misra[3], Kathleen Alexander[3], and Anthony D. Rollett[1]

[1]Carnegie Mellon University, Department of Materials Science & Engineering, PA, USA
[2]Theoretical Division, T-1, Los Alamos National Laboratory, NM, USA
[3]Materials Science and Technology, MST-8, Los Alamos National Laboratory, NM, USA

ABSTRACT

It is known that by controlling microstructural development, desirable properties of materials can be achieved. The main objective of our research is to understand and control interface dominated material properties, and finally, to verify experimental results with computer simulations. We have previously showed a strong similarity between small-scale grain growth experiments and anisotropic three-dimensional simulations obtained from the Electron Backscattered Diffraction (EBSD) measurements [1]. Using the same technique, we obtained 5170-grain data from an Aluminum-film (120μm thick) with a columnar grain structure. Experimentally obtained starting microstructure and grain boundary properties are input for the three-dimensional grain growth simulation. In the computational model, minimization of the interface energy is the driving force for the grain boundary motion. The computed evolved microstructure is compared with the final experimental microstructure, after annealing at 550 ºC.

INTRODUCTION

Characterization of the structures and properties of grain boundary networks (GBN) to produce desirable microstructures is one of the fundamental problems in interface science. There is an ongoing research for the development of new experimental and analytical techniques in order to obtain and synthesize information related to GBN ([2]; [3]; [4]). The grain boundary energy and mobility data were characterized by Electron Backscattered Diffraction (EBSD) technique and Atomic Force Microscopy (AFM) observations (i.e., for ceramic MgO [5] and for the metal Al [6]). Grain boundary energies are extracted from triple junction (TJ) geometry considering the local equilibrium condition at TJ's [7]. Relative boundary mobilities were also extracted from TJ's through a statistical/multiscale analysis [8]. Additionally, there are recent theoretical developments [9] of grain boundary evolution in microstructures.

In this paper, a new technique for three-dimensional grain growth simulations was used to simulate interface migration by curvature driven motion [10]. This method utilizes gradient-weighted moving finite elements (GWMFE) combined with algorithms for performing topological reconnections on the evolving mesh. We have previously showed a strong similarity between small-scale grain growth experiments and anisotropic three-dimensional simulations [1] obtained from the EBSD measurements [11]. Using the same technique, we obtained 5170-grain data from a thin Aluminum film with a columnar grain structure and compared the computational results with experiments.

SIMULATION WITH GRAIN3D CODE

Grain3D is a microstructure evolution code where grain boundaries migrate by mean curvature motion, by using gradient-weighted moving finite elements (GWMFE) in three dimensions. The code assumes that the grain boundary motion is proportional to the local mean curvature of the interface.

$$v_n = \mu\sigma K \tag{1}$$

where v_n is the normal velocity of the interface, K is the curvature, μ is the mobility of the grain boundary, σ is the interface energy per unit area. K is the sum of principal curvatures, i.e., twice the mean curvature. Time dependent solution of grain migration is obtained by minimizing the function,

$$\int (v_n - \mu\sigma K)^2 \, dS \tag{2}$$

over all possible values for the derivatives $\dot{x}_i$.(The integral is over the surface area of the interfaces). Using (2), we obtain a system of 3N ODEs (for detailed analysis, see [10]):

$$\left[\int \hat{n}\hat{n}^T \alpha_i \alpha_j dS \right] \dot{x}_j = \int \mu\sigma K \hat{n} \alpha_i dS \tag{3}$$

where $x = (x_1, x_2, \ldots x_N)^T$ is the 3N-vector containing the x ,y ,and z coordinates of all N interface nodes. The ODEs are solved with an implicit second order backwards difference variable time-step ODE solver.

Several steps are required in order to generate an input for the simulation from EBSD experiment result. First, an image is recorded by secondary electron or backscattered contrast and corrected for instrumental distortions. The image analysis algorithm then locates the grain boundaries and the triple junctions. This information is essential for the mesh generation and characterization of the morphology and topology of the grain boundary network. Meshing is accomplished by a grid generation algorithm (Los Alamos Grid Toolbox-LaGrit [12]), which simultaneously interacts with the microstructural evolution computer code (Grain3d). In the next sections, a brief description of grain boundary skeletonization is explained.

MORPHOLOGICAL ANALYSIS OF GRAIN BOUNDARIES

Pattern analysis and computer information is essential to transform information from experimental data into computer simulation input. There are several algorithms to locate the grain boundaries. One novel method used in this paper is based on the use of unstructured grids. In particular, the Chordal Axis Transform (CAT) is applied to a Delaunay tessellation of boundary pixel enclosing contours [13]. The CAT generates a skeleton of the boundary pixel set

as follows: When a shape is discretized, its boundary is described by a set of edges. A constrained Delanuay tessellation is applied to the edges point set and the edges yielding a unique unstructured grid. The triangles, which are formed by this method, carry structural information of the shape, i.e., information about junctions, prolongations and/or terminations. These structural elements allow for an introduction of a shape graph (skeleton), which describe the morphology of that shape (grain boundaries). The resulting skeleton is connected by grid elements. Nodes are then distributed on the surfaces from the experimental boundary information. Finally, the nodes are connected into volume elements. Figure 1A demonstrates an experimental input (columnar Al-foil), which is skeletonized by CAT algorithms and then meshed for computer input.

ENERGY AND MOBILITY DEPENDENCE OF INTERFACE MOTION

Interface mobility and energy depend on the misorientation between the adjacent grains. They have been measured recently for this same material [6] and these experimental values listed in Table 1 have been incorporated into the Grain3D code.

Misorientation Angle	<3	3-4	4-5	5-6	6-7	7-8	8-9	9-10	10-11	11-12	12-13	13-15	>15
Energy	0.15	0.16	0.20	0.22	0.25	0.26	0.25	0.30	0.31	0.32	0.34	0.35	0.37
Mobility	0.03	0.004	0.04	0.02	0..03	0.006	0.009	0.01	0.05	0.25	0.28	0.40	0.83

Table 1. Grain boundary energy and mobility values for Al-foil

A general question between any experimental results and computational simulations is how to compare them quantitatively. For this purpose, we introduced "the spatial energy function" which is a way of comparing experiment and computation. The initial and final configuration of the experimental microstructure is triangulated and meshed with the techniques that are described in the previous sections. Initial experimental microstructure data is used as input to the computational model and this input is used for the simulation (Figure 1C). Three different simulations are performed with the interface parameters. In the first one, the boundary mobility and energy are assumed constant and equal to unity (isotropic simulation). For the second case, the mobility is assumed to be dependent on the misorientation angle (anisotropic simulation with mobility). The last case is where both mobility and energy are variables of misorientation. Several snapshots are taken from the integration of the simulations and they are compared with the final configuration of the experiment. A quantitative measure for the comparison is given by a spatial energy function,

$$E_i = \frac{1}{Z} \sum_{x,y} 1 - \delta\left[s_i(x,y) - s_{ref}(x,y)\right] \tag{4}$$

where E_i is the energy for snapshot i (i = 1,2…,n and n is the total number of snapshots for the whole simulation), s_i is the crystal orientation for the i^{th} snapshot of the simulation, and s_{ref} is the crystal orientation for the reference state (final configuration), δ is the delta function, and Z is

the normalization constant. If the crystal orientation for the spatial point (x,y) is same as the reference crystal orientation of the same (x,y) location, then the energy for this configuration does not change and the delta function is zero, otherwise it is one. The total energy for the i^{th} configuration is then given by summing over the total area for all (x,y) points. One can easily see a similarity between our spatial energy function and magnetic spin states calculation. Figure 2 shows the results for isotropic and anisotropic simulation results. In the isotropic case, the spatial energy function diverges; whereas the anisotropic mobility case reaches a minimum around time step 30.

Interface velocity depends on both energy and mobility values but the energy values are also important for the determination of dihedral angles. If there is no dependence on energy, then the dihedral angles are 120°. However, if the energy depends on misorientation, then the dihedral angles are determined by the sine law of relative energy values. Therefore, energy dependence of misorientation introduces a new constraint. Figure 2 shows the results of simulating grain growth with both anisotropic energy and mobility. In this case, although the simulation results diverge from the experiment, there is a shallow minimum at t=13.

Absolute grain boundary mobility values have been measured for a wide variety of materials and boundary types by Gottstein [14]. For aluminum bi-crystals they found reduced mobilities (i.e. the product of mobility with energy) in the range 10^{-8} to 10^{-7} m^2/s for two similar types of high angle boundaries and various purities [14] at 547°C. In the grain growth experiment described here, the crude estimate of mean curvature is of order 0.001 μm^{-1} (for example, assume grains with 100 μm radius, then the curvature will be 0.01 μm^{-1}, but because of the triple junctions one may deduce much lower curvature, say 0.001μm^{-1}). Based on the range of (reduced) mobilities observed by Gottstein *et al*., a migration rate of approximately $v=\mu\sigma\kappa=1.10^{-8}$ m^2/s 0.001μm^{-1} = 10 μm/s is expected. This migration rate is high when compared to the estimated migration rates in our experiment (an estimated migration rate is 100μm / 1000s = 0.1 μm/s). We note, however, that the purity of the material used in the bi-crystal experiments (99.9998 %) was significantly higher than that in our experiments (99.98% pure). Also, note that the Gottstein *et al.* measurements were for high angle boundaries whereas the majority of boundaries in this experiment were low angle boundaries with significantly lower average mobility. For comparison of simulation times with experiment, these values can be used to estimate the migration distance during annealing at various temperatures.

DISCUSSION AND CONCLUSION

The comparison between the experiment and computed results provides important details related to grain evolution. A strong similarity is observed between growth experiments and anisotropic three-dimensional GWMFE simulations. It is clear from the simulation results that anisotropy in the grain boundary energy and mobility has a major effect on the growth process and the growth is driven by these parameters.

There are several advantages of quantitative comparison of experiment and simulation. From Figure 2, we can conclude from y-axis that there is 80% agreement between experimental microstructure and computational output. From time-axis (x-axis), we can also obtain real time correspondence of experiment. In our case, the energy function reaches a minimum around time equal to 30.

In Figure 3, the number of facet distribution for the initial experimental microstructure of the Aluminum film is given (5170 grain). This information is useful for the determination of the average behavior of microstructural evolution. Extension of this work to calculate the statistical averages is in preparation. Finally, we conclude that the present simulation method verified the experimentally determined microstructure in large-scale simulations.

ACKNOWLEDGMENTS

This work was supported by the MRSEC program of NSF under award number DMR-0079996 and Department of Energy under Contract W-7405-ENG-36.

REFERENCES*

1. M. C. Demirel, A. P. Kuprat, D. C. George, G. B. Straub, A. D. Rollett, *Interface Science* **10**, 139 (2002).
2. B. L. Adams, *Ultramicroscopy* **67**, 11-17 (1997).
3. R. M. Suter, K. Kosack, Proceedings of the twelfth international Conference on Texture of Materials, Montreal, Canada (1999), pp. 80-85.
4. D. J. Jensen, A. Kvick, E. M. Lauridsen, U. Lienert, L. Margulies, S. F. Nielsen, H. F. Poulsen, Plastic deformation, recrystallization and internal stresses studied by a new 3D X-Ray microscope, MRS Fall'99 Meeting, Boston, MA, USA (1999), pp. 227-240.
5. D. Kinderlehrer, I. Livshits, D. Mason, S. Ta'asan, *Interface Science* in press (2002).
6. C.-C. Yang, W. W. Mullins, A. D. Rollett, *Scripta Materialia* **44**, 2735-2740 (2001).
7. B. L. Adams, D. Kinderlehrer, W. W. Mullins, A. D. Rollett, S. Ta'asan, *Scripta Materialia* **38**, 531- 536 (1998).
8. D. Kinderlehrer, I. Livshits, S. Ta'asan, D. E. Mason, Multiscale reconstruction of grain boundary energy from microstructure, Twelfth International Conference on Textures of Materials, Montréal, Canada (1999), pp. 1643 - 1648.
9. W. W. Mullins, *Acta Metallurgica* **37**, 2979-2984 (1989).
10. A. Kuprat, *Siam Journal on Scientific Computing* **22**, 535 - 560 (2000).
11. M. C. Demirel, B. S. El-Dasher, B. L. Adams, A. D. Rollett, in *Electron Backscatter Diffraction in Materials Science* M. K. Adam J. Schwartz, and Brent L. Adams, Ed. (Kluwer Academic/Plenium Publishers, New York, 2000) pp. 65 - 74.
12. D. George, User Manual, http://www.t12.lanl.gov/~lagrit/. (1995).
13. B. R. Schlei, Region enclosing contours from edge pixels, SPIE conference proceedings, Seattle (2002), in print.
14. G. Gottstein, L. S. Shvindlerman, (CRC Press, Boca Raton, 1999).

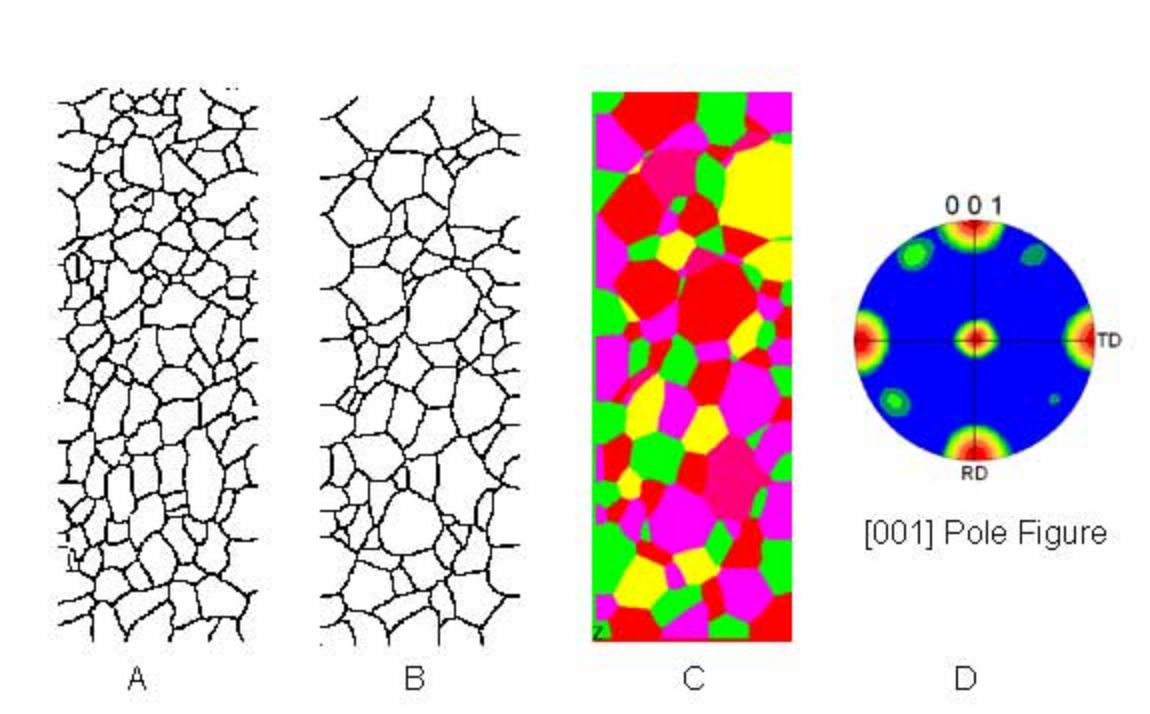

Figure 1. A) Initial experimental microstructure (top view) with dimensions 900μmx2500 μm, B) Final experimental microstructure, C) Simulated microstructure, D) A strong cube texture is observed from [001] Pole figure

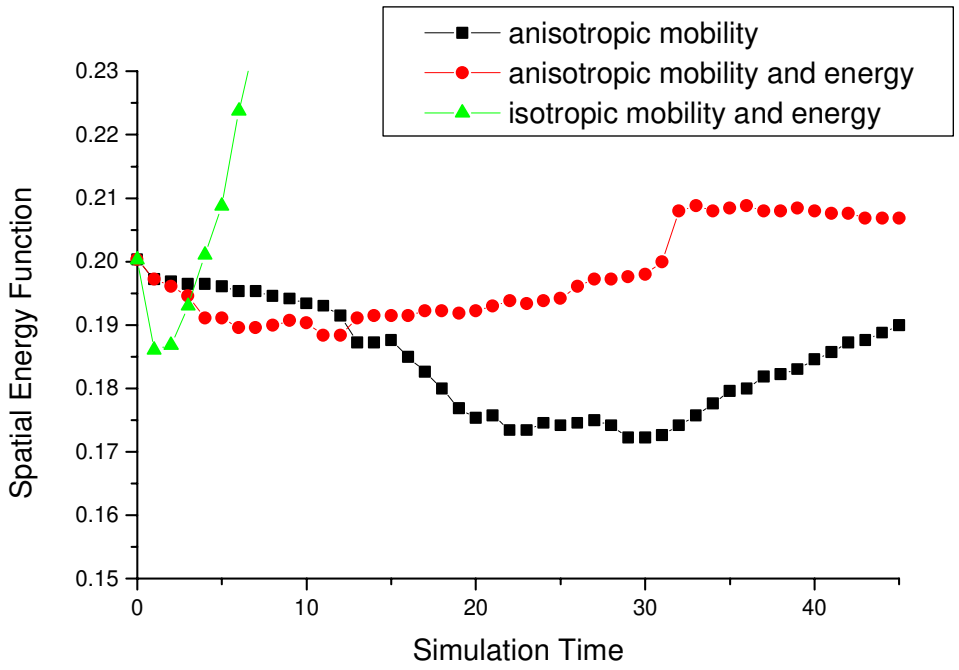

Figure 2. Simulation results with energy and mobility parameter: isotropic case (green curve) diverges to energy value of one (the values bigger then 0.23 not shown); anisotropy due to both mobility and energy (red) which reaches a shallow minimum at t=13; anisotropy due to mobility only (black) which reaches a minimum around t= 30

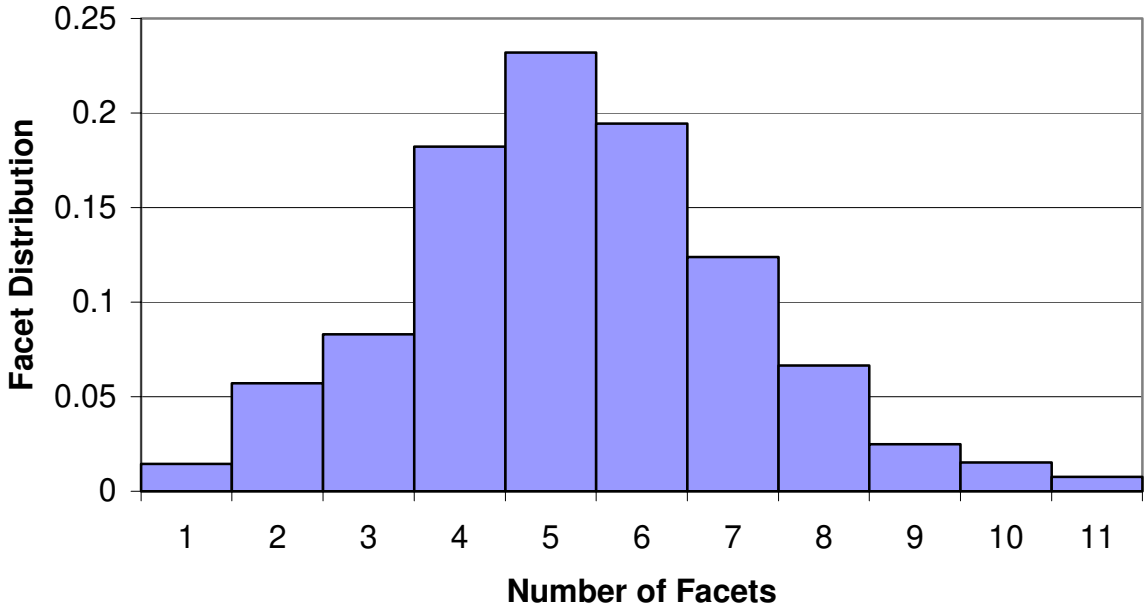

Figure 3. Statistical data from experiment: Number of facet distribution in the initial experimental microstructure of the Aluminum film.